MITF Modulates Therapeutic Resistance through EGFR Signaling

Zhenyu Ji[1], Yiyin Erin Chen[1], Raj Kumar[1], Michael Taylor[1], Ching-Ni Jenny Njauw[1], Benchun Miao[1], Dennie T. Frederick[2], Jennifer A. Wargo[3], Keith T. Flaherty[2], Göran Jönsson[4] and Hensin Tsao[1,2]

Response to targeted therapies varies significantly despite shared oncogenic mutations. Nowhere is this more apparent than in BRAF (V600E)-mutated melanomas where initial drug response can be striking and yet relapse is commonplace. Resistance to BRAF inhibitors have been attributed to the activation of various receptor tyrosine kinases (RTKs), although the underlying mechanisms have been largely uncharacterized. Here, we found that EGFR-induced vemurafenib resistance is ligand dependent. We employed whole-genome expression analysis and discovered that vemurafenib resistance correlated with the loss of microphthalmia-associated transcription factor (MITF), along with its melanocyte lineage program, and with the activation of EGFR signaling. An inverse relationship between MITF, vemurafenib resistance, and EGFR was then observed in patient samples of recurrent melanoma and was conserved across melanoma cell lines and patients' tumor specimens. Functional studies revealed that MITF depletion activated EGFR signaling and consequently recapitulated the resistance phenotype. In contrast, forced expression of MITF in melanoma and colon cancer cells inhibited EGFR and conferred sensitivity to BRAF/MEK inhibitors. These findings indicate that an "autocrine drug resistance loop" is suppressed by melanocyte lineage signal(s), such as MITF. This resistance loop modulates drug response and could explain the unique sensitivity of melanomas to BRAF inhibition.

Journal of Investigative Dermatology (2015) **135,** 1863–1872; doi:10.1038/jid.2015.105; published online 9 April 2015

INTRODUCTION

Primary and secondary resistance to molecular therapies remains a cardinal challenge in the clinical setting. For metastatic melanoma, the pace of progress from the benchside discovery of BRAF (V600E) to the bedside delivery of vemurafenib (VEM) has been rapid. As with other targeted agents, however, acquired resistance to selective BRAF inhibitors (SBIs) soon followed on the heels of clinical success. COT expression (Johannessen *et al.*, 2010), SOX10 reduction (Sun *et al.*, 2014), *BRAF* amplification (Shi *et al.*, 2012), splice variation (Poulikakos *et al.*, 2011), *NRAS* mutagenesis, and receptor tyrosine kinase (RTK) activation (Nazarian *et al.*, 2010; Villanueva *et al.*, 2010; Yadav *et al.*, 2012; Girotti *et al.*, 2013) have all been linked to SBI resistance in melanoma. Although these mechanisms all confer a similar phenotype of mediating cell survival and proliferation, the relative contribution of subclonal selection versus epigenetic reprogramming of cell state to the emergence of each mechanism is not known. On the other hand, the lineage dependency of SBI sensitivity suggests that cellular differentiation state might underlie any of the previously described mechanisms of resistance to SBIs.

We thus set out to characterize changes in transcriptional programming that occur during the course of *in vitro* selection for VEM resistance. Using a forward pharmacogenetic screen, we discovered that VEM resistance was associated with different degrees of cellular reprogramming. On one hand, resistance that emerges from a BRAF splice product is associated with minimal changes in cell state. On the other hand, resistance can also be associated with significant transcriptome changes anchored by the concomitant loss of the master melanocyte lineage regulator, microphthalmia-associated transcription factor (MITF), with the activation of EGFR, a pathway little utilized in these neural crest–derived cells. We show that modulating MITF levels alters VEM sensitivity in both melanoma and colon cancer, and that a reciprocal relationship between MITF and EGFR is conserved across melanoma specimens and correlates with VEM response. Our studies point to lineage identity as a major determining factor for SBI sensitivity.

[1]*Wellman Center for Photomedicine/Department of Dermatology, Massachusetts General Hospital, Harvard Medical School, Boston, Massachusetts, USA;* [2]*MGH Cancer Center, Massachusetts General Hospital, Boston, Massachusetts, USA;* [3]*Surgical Oncology and Genomic Medicine, The University of Texas MD Anderson Cancer Center, Houston, Texas, USA and* [4]*Department of Clinical Sciences Lund, Division of Oncology and Pathology, Lund University, Lund, Sweden*

Correspondence: Hensin Tsao, Massachusetts General Hospital and Harvard Medical School, Wellman Center for Photomedicine, Edwards 211, 55 Fruit Street, Boston, 02114-2696, Massachusetts, USA.
E-mail: htsao@mgh.harvard.edu

Abbreviations: cDNA, complementary DNA; GI_{50}, 50% growth inhibition; HB-EGF, heparin-binding EGF; MEK, mitogen-activated protein kinase (MAPK)/extracellular signal–regulated kinase (ERK) kinase; MITF, microphthalmia-associated transcription factor; RTK, receptor tyrosine kinase; SBI, selective BRAF inhibitor; siRNA, small interfering RNA; VEM, vemurafenib

Received 18 December 2014; revised 11 February 2015; accepted 27 February 2015; accepted article preview online 19 March 2015; published online 9 April 2015

RESULTS

In order to elucidate programmatic changes that occur with VEM resistance, we subjected two melanoma cell lines, A375 and SKmel-28, to escalating doses of VEM in order to generate isogenically matched pairs of sensitive and resistant cell lines. Dose interrogation showed that both resistant cell lines (i.e., A375R and SKmel-28R exhibited >10-fold increase in their VEM 50% growth inhibition GI_{50}s; Figure 1a) compared with their parental counterparts. Both resistant lines showed increased $pAKT^{473}$ and reengagement of mitogen-activated protein kinase signaling, although the A375R cells retained sensitivity to MEK (mitogen-activated protein kinase/

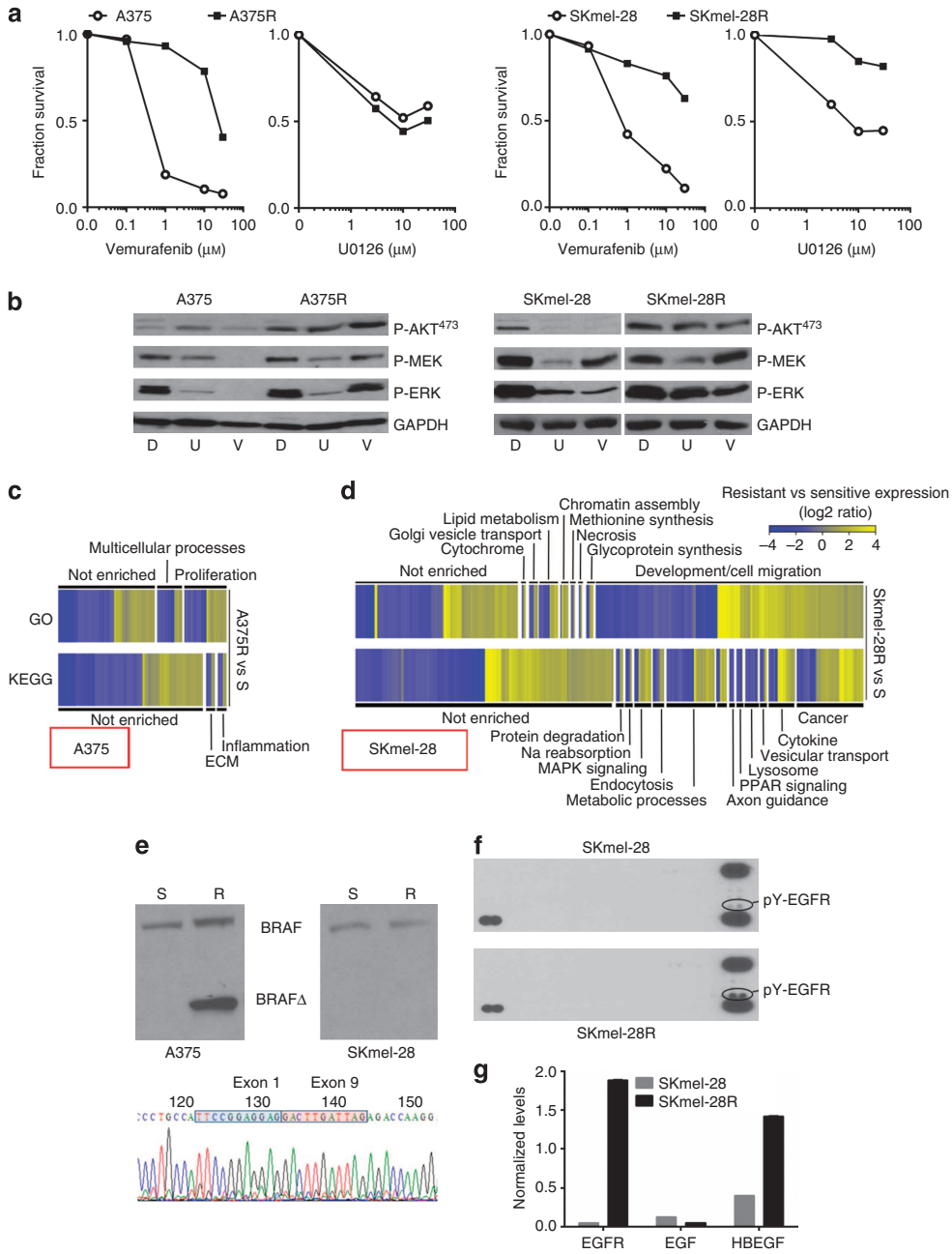

Figure 1. Characteristics of vemurafenib (VEM)-resistant lines. (**a**) A375R and SKmel-28R cells (closed squares) showed >10-fold increase in VEM GI_{50} (50% growth inhibition) compared with their parent cell lines (open circles). SKmel-28R, but not A375R, are also crossresistant to MEK (mitogen-activated protein kinase (MAPK)/extracellular signal–regulated kinase (ERK) kinase) inhibitor U0126 (5 μM). (**b**) Kinase signaling responses to DMSO control (labeled D), U0126 (U; 5 μM), and VEM (V; 5 μM) in A375, A375R, SKmel-28, and SKmel-28R lines. Gene Ontology (GO) and Kyoto Encyclopedia of Genes and Genomes (KEGG) analyses for differentially expressed genes between (**c**) the A375 and A375R pair and between (**d**) the SKmel-28 and SKmel-28R pair (**e**). A375R cells harbor a BRAFΔ2-8 splice variant that is not present in either the native A375 cells or the SKmel-28/SKmel-28R pair. (**f**) Phosphotyrosine (pY)-receptor tyrosine kinase (RTK) blot analysis shows increased pY-EGFR in the SKmel-28R cells as compared with the SKmel-28 cells, whereas (**g**) quantitative PCR (qPCR) analysis reveals upregulation of *HB-EGF* and *EGFR*, but not *EGF*, in the SKmel-28R line.

extracellular signal–regulated kinase (ERK) kinase) inhibition, whereas SKmel-28R developed cross-resistance (Figure 1a and b). We subsequently subjected all four sets of cell lines in triplicate to comparative gene expression analysis.

Profiling of the A375 versus A375R pair revealed strikingly sparse gene expression changes associated with the gain of VEM resistance (Supplementary Figure S1 online). Of the 12,466 species surveyed, only 0.37% and 0.52% showed >2-fold induction and suppression, respectively, with maximum changes ranging from a 5.8-fold induction of *MAGEA1* to a 6.7-fold suppression of *SERPINA3* (Supplementary Table S1 online). Gene Ontology (GO) and KEGG (Kyoto Encyclopedia of Genes and Genomes) categories affected by these minor expression variations (Figure 1c) included "proliferation" (GO) and "inflammation" and "ECM" (KEGG). As the A375R cells retained sensitivity to MEK inhibitors (Figure 1a and b), we hypothesized that the resistance lesion was upstream of MEK. Exome sequencing (Supplementary Table S2 online) did not detect any acquired mutations in *NRAS*, *HRAS*, *KRAS*, *MAP2K1*, *MAP2K2*, *CRAF*, or *BRAF*, although there was a BRAF(Δ2-8) splice variant that was present in the A375R but not the A375 parent line (Figure 1e). This specific alteration has been reported in a VEM-resistant human tumor specimen (patient no. 5 from a recent report (Poulikakos *et al.*, 2011)) and therefore is likely driving VEM resistance in A375R cells.

In contrast to the A375 pair, expression analysis of SKmel-28 versus SKmel-28R revealed significant programmatic changes with the emergence of VEM resistance (Supplementary Figure S1 online). Overall, 3.4% and 3.0% of the genes exhibited a >2-fold increase or decrease, respectively, with a dynamic range of 114-fold induction (*IL1B*) and 57-fold suppression (*LOC728715*, Supplementary Table S1 online). GO analysis indicated major shifts in "development/cell migration" genes whereas KEGG categorization yielded numerous enrichments including "cancer", "cytokine", and "metabolic processes" (Figure 1d). The SKmel-28R cells lacked putative BRAF splice variants (Figure 1e) and differed from the A375R cells in demonstrating coresistance to both VEM and MEK inhibition (Figure 1a and b). Comparative phosphotyrosine RTK blot analysis of the SKmel-28 and SKmel-28R pair uncovered sustained EGFR signaling on SKmel-28R cells (Figure 1f) that has been reported to cause VEM resistance (Corcoran *et al.*, 2012; Girotti *et al.*, 2013). There is no dramatic alteration of phospho-EGFR in A375R (Supplementary Figure S1C). Additional exome sequencing of SKmel-28 and SKmel-28R did not reveal biologically plausible acquired variants in *EGFR*, *NRAS*, *HRAS*, *KRAS*, *MAP2K1*, *MAP2K2*, *CRAF*, or *BRAF* (Supplementary Table S2 online). Taken together, these results suggest that direct target modification, such as the BRAF splice product in A375R cells, neutralizes drug effects by resetting a specific signaling pathway but leaves few programmatic footprints. In contrast, EGFR activation in SKmel-28R cells appears to be associated with more profound gene expression alterations. We thus set out to clarify the mechanism by which EGFR may have become activated in the SKmel-28R cells.

As growth factors and cytokines are well-known activators of RTK signaling, we first interrogated these genes in the microarray and found that a surprising number was upregulated during the gain of resistance in SKmel-28. Among candidate ligand–RTK pairings, *HB-EGF-EGFR and GAS6-AXL* levels were all increased (Supplementary Figure S2 online), although only EGFR appeared to be activated in the phosphotyrosine RTK blot analysis (Figure 1f). Quantitative PCR of SKmel-28R cells confirmed a 39-fold increase in *EGFR* and a 3.5-fold induction of *heparin-binding EGF* (*HB-EGF*) compared with VEM-sensitive SKmel-28 cells (Figure 1g). Thus, an EGFR autostimulatory circuit appears to be selectively sustained and mediating resistance in the SKmel-28R cells.

To experimentally validate the EGFR findings, we generated stable SKmel-28 lines expressing wild-type EGFR, oncogenic EGFR(L858R), or kinase-dead EGFR(D837A) (Figure 2a). In the absence of EGFR ligand, there was only a minimal gain in VEM resistance in EGFR overexpression lines, with the gains in VEM GI_{50}s for SKmel-$28^{EGFR(WT)}$, SKmel-$28^{EGFR(D837A)}$, and SKmel-$28^{EGFR(L858R)}$ cells all <3-fold compared with SKmel-28^{VECTOR} ($GI_{50} = 0.75\ \mu M$). However, on the addition of EGF or HB-EGF, VEM resistance was dramatically enhanced in wild-type EGFR overexpression lines (Figure 2a). There was a 36-fold and a 12-fold increase in VEM GI_{50}s when EGF or HB-EGF, respectively, were exogenously added. As expected, the kinase-inactive EGFR (D837A) allele had minimal effects on VEM resistance even in the presence of EGF or HB-EGF. As both *AXL* and *GAS6* were also upregulated in SKmel-28R compared with SKmel-28 cells in the microarray data, we also transduced *AXL* into SKmel-28 cells. However, we observed only minimal effects on VEM sensitivity either in the absence or presence of exogenous GAS6 (Supplementary Figure S3 online). These results indicate that overexpression of *EGFR* alone may not be sufficient to induce resistance and that ligand upregulation is a critical component of an "autocrine resistance loop".

To elucidate determinants of this resistance loop, we next performed transcriptional factor analysis on differentially expressed genes in SKmel-28R versus SKmel-28 cells (Supplementary Table S3 online). As shown in Figure 2b, MITF suppression was the leading transcriptional footprint with a *Z*-score of -5.391 ($P = 6.37 \times 10^{-39}$); there was also inhibition of SOX10 activity (*Z*-score, -2.153, $P = 2.59 \times 10^{-5}$). These findings are consonant with the categorical change of "development/cell migration" genes, as recovered by GO classification of the microarray data. Validation of the microarray analysis by quantitative PCR and western blotting confirmed dramatic reductions in *MITF* and *MITF-M* along with several downstream MITF targets: *BCL2*, *EDNRB*, and *miR-211* (Figure 2c). Overall, the acquisition of VEM resistance in SKmel-28 cells appears to have silenced the entire melanocytic program as positive upstream MITF regulators (*LEF1*, *PAX3*, and *SOX10*) were all diminished whereas the negative MITF regulator *TCF4* was increased by 420-fold (Figure 2c).

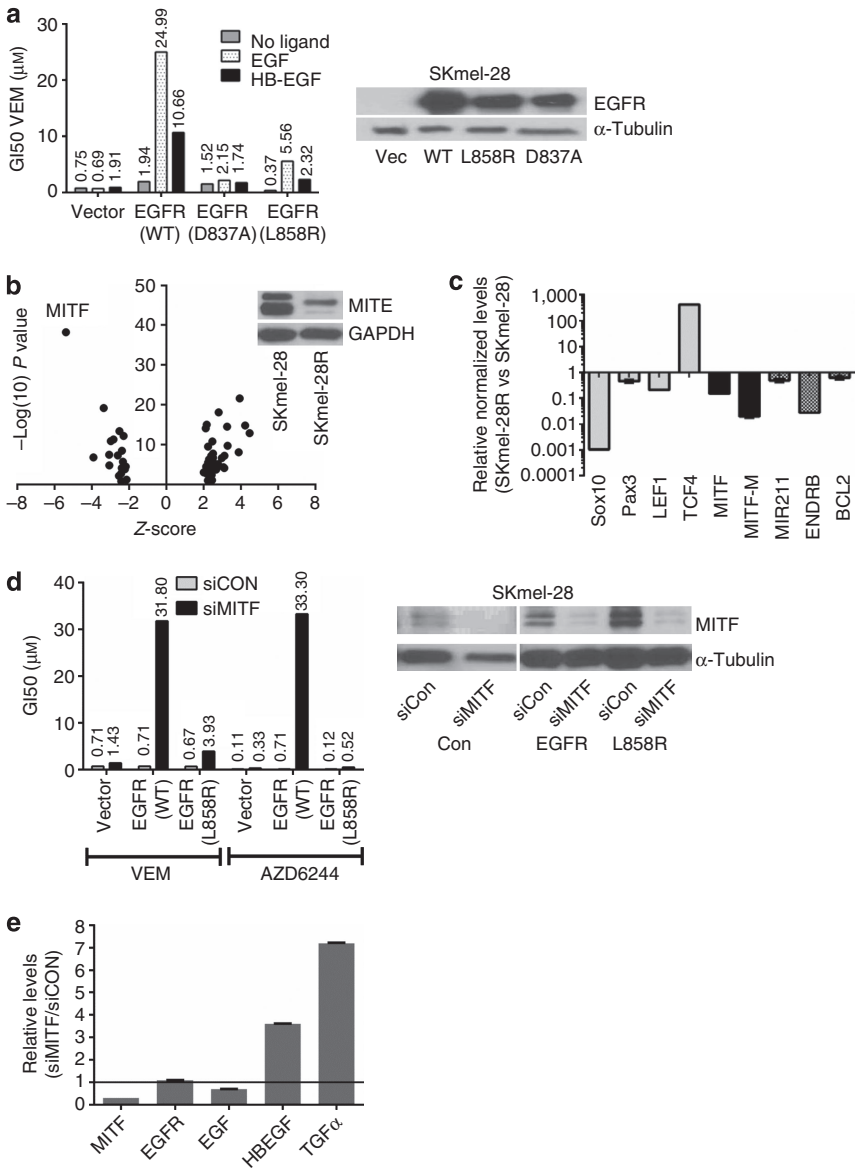

Figure 2. Loss of microphthalmia-associated transcription factor (MITF) contributes to an EGFR autocrine-resistance loop in SKmel-28R cells. (**a**) Stable expression in SKmel-28 cells of EGFR (wild-type (WT)) or EGFR (L858R), but not kinase-dead EGFR (D837A), leads to vemurafenib (VEM) resistance in the presence of exogenously added EGF (10 ng ml^{-1}) or heparin-binding EGF (HB-EGF; 10 ng ml^{-1}), but not in the absence of ligand. Expression of EGFR alone does not significantly increase VEM resistance. (**b**) Using the Ingenuity software, transcription factor analysis of genes differentially expressed between SKmel-28 and SKmel-28R indicate a strong suppression of MITF target genes. Western blotting confirms the loss of MITF protein in SKmel-28R cells (inset). (**c**) Quantitative PCR (qPCR) shows loss of MITF expression in SKmel-28R cells along with that of other melanocytic lineage regulators (*SOX10*, *PAX3*, *LEF1*) and various MITF targets (*MITF-M*, *MiR211*, *ENDRB*, *BCL2*). Levels of *TCF4* (*ITF2*), which is known to suppress MITF (Furumura *et al.*, 2001), is greatly elevated. (**d**) The small interfering RNA (siRNA)–mediated depletion of MITF (denoted siMITF) in stable SKmel-28$^{EGFR(WT)}$ and SKmel-28$^{EGFR(L858R)}$ cells leads to enhanced VEM and AZD6244 resistance even in the absence of EGFR ligand. (**e**) RNA levels of *HB-EGF* and *TGFα*, two known ligands of EGFR, are increased in SKmel-28 cells where MITF has been depleted by siRNA. Thus, loss of MITF closes the "autocrine resistance loop" in the face of higher EGFR expression. Numbers above columns represent actual GI_{50} (50% growth inhibition) values.

To determine whether MITF loss cooperates with EGFR activation in mediating resistance, we depleted MITF in the stable EGFR SKmel-28 lines (Figure 2d) using small interfering RNA (siRNA) and observed the acquisition of strong resistance against both VEM (45-fold increase in GI_{50}) and AZD6244 (300-fold increase in GI_{50}) in the SKmel-28$^{EGFR(WT)}$ cells even in the absence of EGFR ligand (Figure 2d). The siRNA-mediated depletion of MITF had no acute effects on the amount of EGFR and EGF but did immediately increase the levels of HB-EGF (3.6-fold) and transforming growth factor-α (7.2-fold), both of which are known ligands for EGFR (Figure 2e). In addition, neuregulin 1, an indirect activator of EGFR through ERBB4 or ERBB3 binding, was also increased 5.1-fold after MITF knockdown (data not shown). These

findings indicate that MITF suppression may create an autocrine ligand-rich environment that synergizes with EGFR upregulation to mediate resistance.

In order to independently replicate the MITF/EGFR observation, we generated additional pairs of VEM-sensitive and -resistant melanoma cell lines and found that the emergence of VEM resistance in another line, MGH-CH1, was also correlated with MITF loss and EGFR activation (Supplementary Figure S4a and b online). Using the aforementioned strategy, we stably introduced EGFR (WT), EGFR (L858R), and EGFR (D837A) alleles into MGH-CH1 cells and assessed VEM sensitivity. As shown in Supplementary Figure S4c online, both MGH-CH1$^{EGFR(WT)}$ and MGH-CH1$^{EGFR(L858R)}$ cells exhibited ligand-dependent VEM resistance compared with MGH-CH1^{vector} and MGH-CH1$^{EGFR(D837A)}$ cells, consistent with the SKmel-28 results. Next, suppression of MITF in MGH-CH1$^{EGFR(L858R)}$ cells also led to a gain of resistance to both VEM and AZD6244 in the absence of ligand (Supplementary Figure S4d online). In contrast to SKmel-28 cells, however, the EGFR (L858R) allele seemed to play a stronger role than wild-type EGFR in the MGH-CH1 cells.

We next sought broader evidence of an interaction between levels of *MITF*, *EGFR*, and therapeutic sensitivity. First, we examined the CCLE (Cancer Cell Line Encyclopedia) database (Barretina *et al.*, 2012) and found significant correlations (Figure 3a) between PLX4720 resistance and low *MITF* ($P=0.001$), high *EGFR* ($P=0.0001$), low *LEF1* ($P=0.025$), and high *TCF4* ($P=0.011$); PLX4720 insensitivity was marginally related to low *SOX10* ($P=0.078$) but not to *PAX3* ($P=0.76$). In addition, copy number analysis using a set of BRAF(V600E) melanoma lines (Ji *et al.*, 2012) revealed that MITF amplification is associated with increased sensitivity to both VEM and the MEK inhibitor U0126 (Supplementary Figure S5 online), further strengthening the role of MITF in melanoma's response to mitogen-activated protein kinase pathway inhibition. Thus, the pattern of lineage silencing, high *EGFR*, and SBI insensitivity appears to be preserved across a panel of melanoma lines. We next set out to confirm the relationship between acquired VEM resistance and MITF levels in tumor specimens. We first examined changes in MITF expression using a publicly available microarray data set (Gene Expression Omnibus (GEO) GSE50509) that captured gene expression data for 20 pretreatment and 30 relapse melanoma specimens from 20 patients. As shown in Figure 3b, the majority of relapsed tumors showed evidence of MITF loss. As *EGFR* probes in GSE50509 did not pass our quality filter, we also verified trends in *MITF* and *EGFR* expression by quantitative PCR using an in-house collection of BRAF (V600E)-mutated tumors from patients treated with BRAF±MEK inhibitors. The average relative $\log_2$-fold change between pre- and post-relapse specimens was −0.88 for *MITF* and 0.61 for *EGFR* (Figure 3c; $P=0.002$). In 4/5 tumor pairs, the relapse specimen had lower *MITF* levels but higher *EGFR* levels compared with the pretreatment samples.

The overall expression patterns that relate both MITF and EGFR to VEM response also suggest that the two molecules may exhibit innate reciprocity. First, a significant negative correlation between MITF and EGFR was identified in the 28 CCLE melanoma lines (Figure 4a; $P<0.0001$). Turning to melanoma specimens rather than cell lines, significant reciprocal relationships were also observed in the 374 tumors ($P<0.0001$) available through The Cancer Genome Atlas (TCGA; Figure 4b and Supplementary Table S4 online) and 31 primary melanomas ($P=0.0005$) and 71 metastatic melanoma specimens ($P=0.0007$) available in the GEO (GSE46517; Figure 4b and Supplementary Table S4). Implicit in these findings is the possibility that MITF may directly counterregulate EGFR signaling. To test this hypothesis, we induced MITF expression for short term in A375 and MGH-CH1 cells using the Tet-on system (Figure 4c). In the A375 cells, there was a modest reduction in EGFR but a complete abrogation of pEGFR. In the MGH-CH1 cells, there was a dramatic loss of EGFR, although basal levels of pEGFR were undetectable. Interestingly, with the acute elevation of MITF levels, there appeared to be a dose-dependent growth retardation in both cell lines (Supplementary Figure S6).

In order to directly assess the drug-sensitizing effects of MITF, we used a set of immortalized primary melanocyte lines (Pmel; Figure 5a) that have stably incorporated BRAF(V600E) alone (Pmel-BRAF*) or both BRAF(V600E) and MITF (Pmel-BRAF*-MITF) together(Garraway *et al.*, 2005). These cells were selected because they harbor the minimal essential elements for defining drug response. As shown in Figure 4a, the native Pmel line had low MITF expression and no BRAF (V600E) as assessed by the VE-1 antibody. EGFR was clearly expressed in both the Pmel and Pmel-BRAF* cells. On the other hand, Pmel-BRAF*-MITF cells had near abolition of EGFR expression. The Pmel-BRAF*-MITF cells were also significantly more sensitive to the selective BRAF inhibitor PLX4720 and MEK inhibitor U0126 (Figure 5b) compared with both Pmel and Pmel-BRAF* cells, suggesting that the addition of MITF conferred enhanced drug sensitivity even in cells with extant BRAF (V600E). We next determined whether MITF can have a similar impact on drug response in nonpigment cells by using a Tet-on MITF system that was engineered into the BRAF (V600E)-mutated HT29 colon cancer line. Forced expression of MITF reduced the levels of pEGFR (Figure 5c) and engendered a >10-fold increase in sensitivity (as measured by GI_{50}s) to both VEM and AZD6244 (Figure 5d). These results support a role for MITF in regulating EGFR and in modulating drug response for both pigment cells and nonpigment cells.

DISCUSSION

Acquired therapeutic resistance in melanoma has been ascribed to various mechanisms. However, the relationship between these acquired lesions and underlying transcriptional programs is not well defined. Our studies suggest that a balance between lineage identity and RTK activation modulates drug sensitivity. More specifically, loss of MITF potentiates an EGFR "autocrine resistance loop" that is not normally utilized by the melanocyte lineage that then mediates therapeutic resistance.

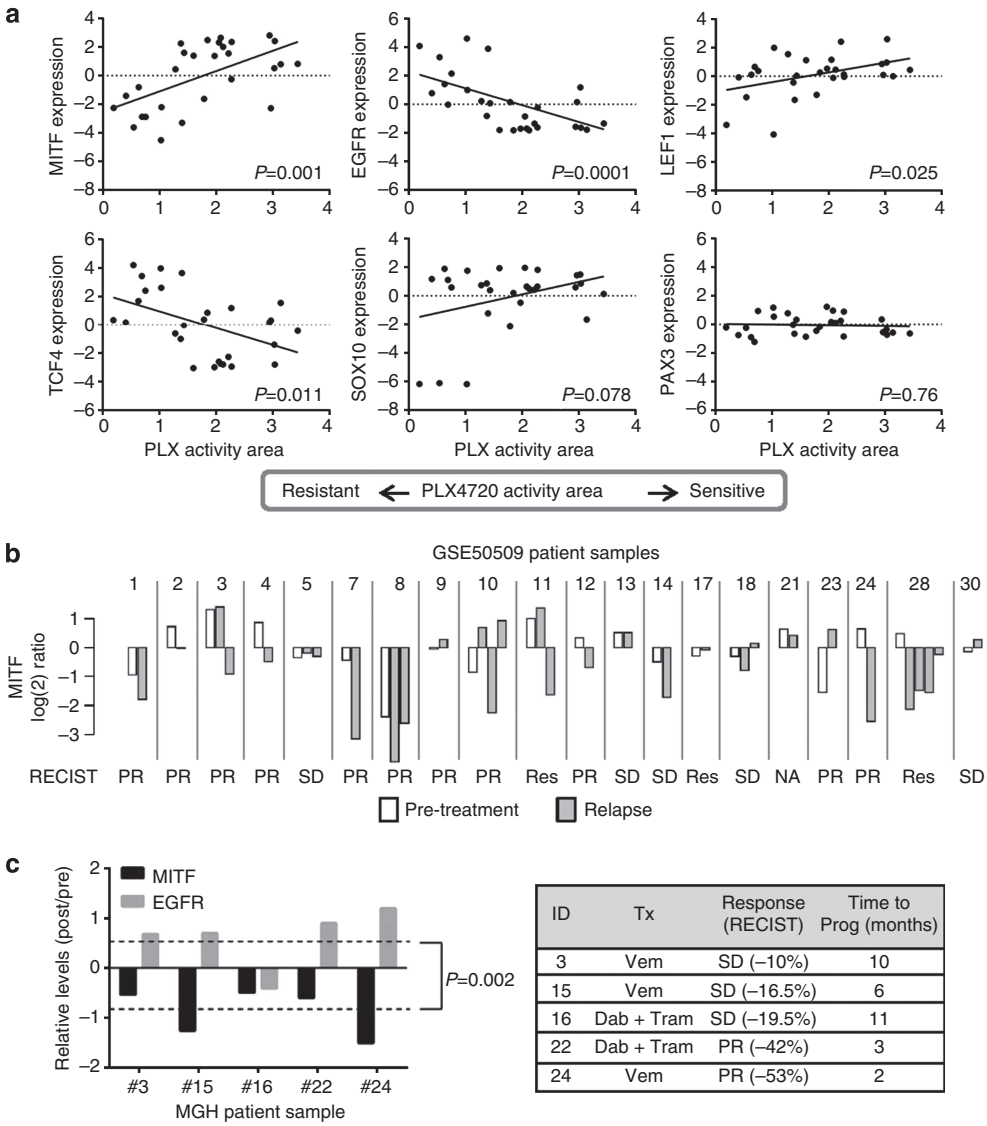

ID	Tx	Response (RECIST)	Time to Prog (months)
3	Vem	SD (–10%)	10
15	Vem	SD (–16.5%)	6
16	Dab + Tram	SD (–19.5%)	11
22	Dab + Tram	PR (–42%)	3
24	Vem	PR (–53%)	2

Figure 3. Expression of the melanocyte lineage program and EGFR correlates with vemurafenib (VEM) sensitivity. (**a**) PLX4720 sensitivity (i.e., increased PLX activity area) is positively correlated with higher *MITF*, *LEF1*, and *SOX10* levels and negatively associated with higher *EGFR* and *TCF4* levels. (**b**) Data from GSE50509 showing microphthalmia-associated transcription factor (MITF) levels in pretreatment (white columns) and postrelapse (gray columns) specimens. Results are shown as $\log_2$ ratios normalized to the mean intensity of pretreatment samples. (**c**) Relative (postrelapse to pretreatment) and normalized (to GUSB) levels of *MITF* and *EGFR* in clinical specimens from patients on BRAF/MEK inhibitor trials. RNA levels were determined by quantitative PCR (qPCR). There is a significant trend toward decreased MITF expression and increased EGFR expression in the postrelapse samples compared with pretreatment samples. Dab, dabrafenib; RECIST, response evaluation criteria in solid tumors; Tx, treatment; Tram, trametinib.

Our analysis of the CCLE data (Barretina *et al.*, 2012), and those of others (Konieczkowski *et al.*, 2014), supports the notion that melanomas with weak lineage identity (low MITF, LEF1, and SOX10) appear to be more resistant to PLX. This hypothesis would harmonize with the rapid ability of colorectal cancers to utilize a lineage-appropriate expression of EGFR to undermine the effects of SBIs in tumors with BRAF mutations (Corcoran *et al.*, 2012; Prahallad *et al.*, 2012). Thus, cells with nominal MITF may predominate during the course of selection. Alternatively, MITF may directly, or indirectly, suppress the EGFR signaling system (Figure 5e) as suggested by our experiments modulating MITF in immortalized melanocytes, melanoma, and colon cancer cells. The use of Pmel cells with stable and genetically defined elements (i.e., BRAF (V600E) and MITF) provides perhaps the most precise and direct evidence that MITF-enriched cells adopt a low-EGFR state that is more drug sensitive. With forced MITF expression in A375 and MGH-CH1 melanomas and HT29 colon cancer cells, there was a direct reduction of EGFR and/or pEGFR.

We also observed an increase in pEGFR with siRNA-mediated MITF depletion but only when cells were stably

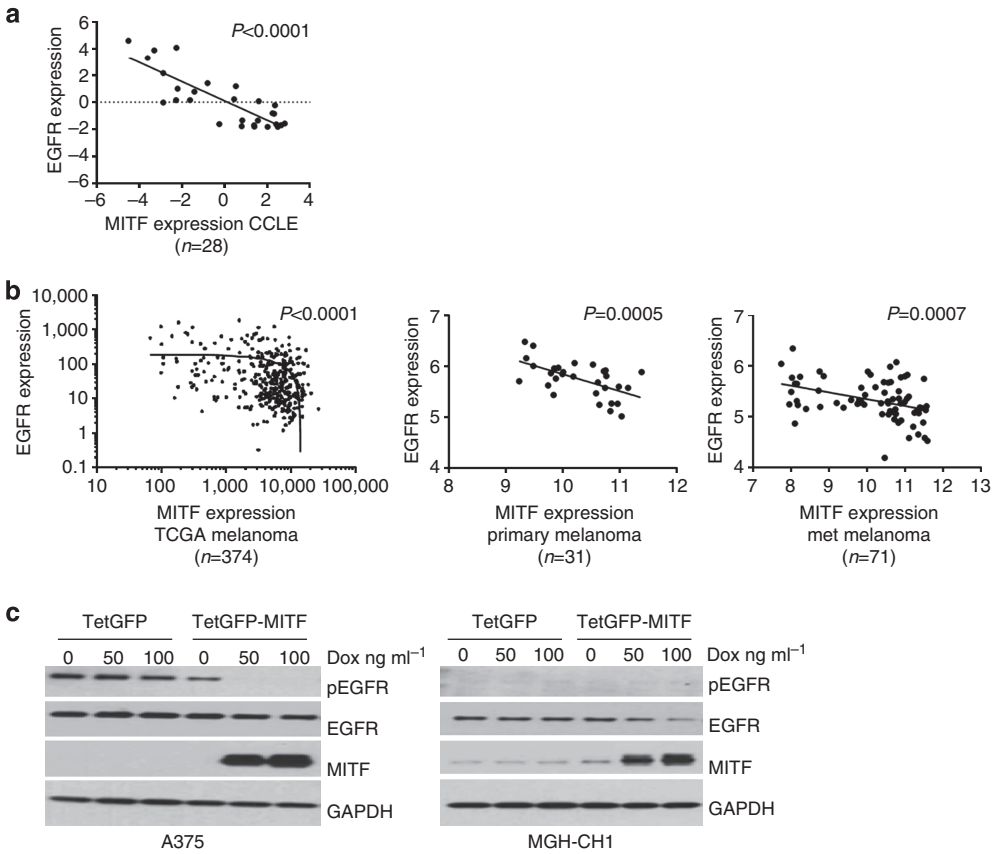

Figure 4. Reciprocity between microphthalmia-associated transcription factor (MITF) and EGFR in melanoma. (**a**) An inverse relationship between levels of *MITF* and *EGFR* can be observed across 28 CCLE (Cancer Cell Line Encyclopedia) melanoma samples and (**b**) 374 melanoma tumor specimens in the TCGA (The Cancer Genome Atlas) and 31 primary melanoma tumors and 71 metastatic (Met) melanoma specimens from GSE46517. Linear regression indicated within dot plot; of note, the TCGA data are plotted in log–log scale and thus the linear regression line appears downwardly curved. (**c**) Induction of MITF in A375 and MGH-CH1 cells using a Tet-on promoter leads to a complete suppression of pEGFR and a slight decrease in EGFR in the A375 cells and a significant decrease in EGFR in the MGH-CH1 cells. Dox, doxycycline.

endowed with ectopic EGFR. Both SKmel-28 and MGH-CH1 lines express robust levels of MITF but exquisitely low levels of EGFR. The prevalence of this phenotype across the melanoma population may explain the markedly higher response rate to SBIs compared with BRAF mutant colorectal cancer. The cooperativity between MITF depletion and overexpression of EGFR and its ligands suggests that MITF loss may contribute to resistance by augmenting levels of ligands, such as HB-EGF and transforming growth factor-α, neuregulin 1, or IL-8, that has reported to be negatively regulated by MITF (Hari Kishore *et al.*, 2012) and that is known to transactivate EGFR (Itoh *et al.*, 2005). Interestingly, a recent report shows that IL-8 signaling can induce chemoresistance by maintaining melanoma-initiating cells (Wilson *et al.*, 2014). Finally, low MITF and high EGFR (and perhaps AXL (Konieczkowski *et al.*, 2014)) could mark exclusive cellular states that harbor distinct therapeutic susceptibilities unrelated to the direct function of these proteins. This static view is supported by the innate reciprocity between MITF and EGFR expression that is preserved across multiple collections of melanoma tumors for which expression data are available (Figure 4a and b). However, the precise mechanism(s) by which MITF interacts with the EGFR signaling system remains the subject of ongoing investigation.

Although there is burgeoning appreciation for a link between melanocyte lineage identity and RTK signaling, there have been several reports examining the role of MITF in dictating drug response. On one hand, Smith *et al.* (2013) found that when A375 cells were induced into resistance against MEK inhibition, emergent subclones exhibited higher MITF and SMURF2 levels. Along these lines, Johannessen *et al.* (2013) used A375 cells in a reverse screen and found that genes in the cAMP pathway induced MITF, strengthened lineage identity, and conferred resistance to RAF, MEK, and ERK inhibitors ; it is worth noting, however, that one of the patient tumors reported in the paper clearly showed loss of MITF with relapse (no. 16; extended data Figure 10d in reference Johannessen *et al.*, 2013). On the other hand, Konieczkowski *et al.* (2014) found that intrinsic PLX resistance is associated with low MITF along with high NF-κB levels. In a related study, Sun *et al.* (2014) also showed that depletion of lineage factor SOX10, but not MITF, increased EGFR and VEM resistance. In that report, sh(MITF) did not alter VEM

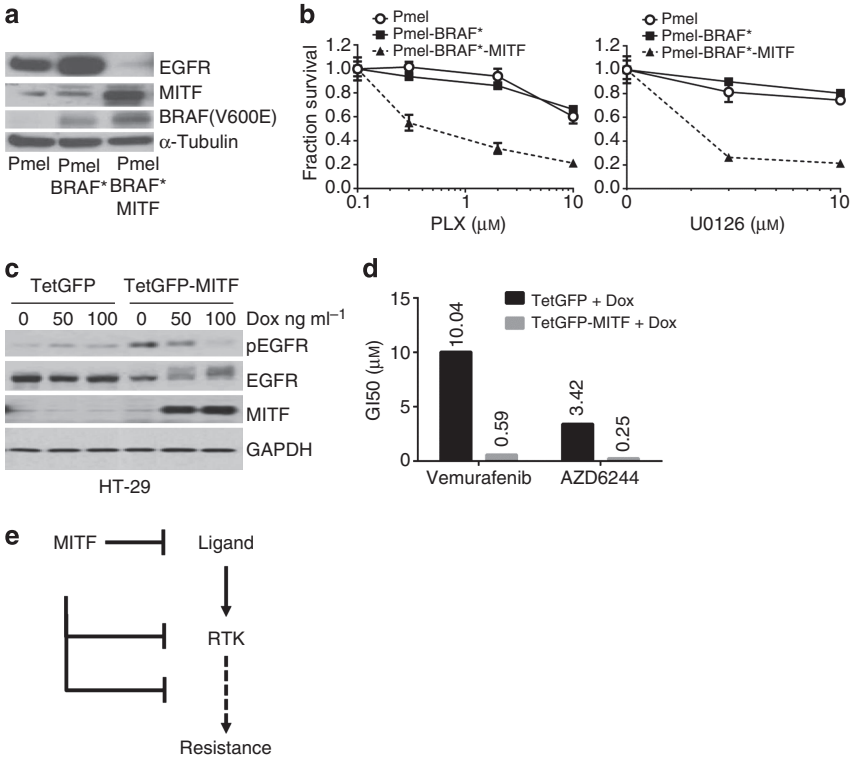

Figure 5. Overexpression of microphthalmia-associated transcription factor (MITF) confers therapeutic sensitivity. (**a**) Immortalized primary melanocytes (Pmel) with stable expression of BRAF (V600E) and MITF (Pmel-BRAF*-MITF) have lower EGFR levels than either control Pmel cells or Pmel cells with only BRAF (V600E) (Pmel-BRAF*). (**b**) Pmel-BRAF*-MITF (solid triangle) cells are more sensitive to both PLX and U0126 than Pmel (open circle) and Pmel-BRAF* (solid squares) cells. (**c**) The colon cancer cell line HT29, which harbors a BRAF(V600E) mutation, was transduced with a Tet-on vector (TetGFP) or Tet-on MITF (TetGFP-MITF) and induced to express MITF using the indicated doses of doxycycline (Dox). (**d**) Induced expression of MITF in HT29 leads to increased sensitivity to vemurafenib and AZD6244, as determined by a >10-fold reduction in the GI_{50} (50% growth inhibition). (**e**) One possible model suggests that MITF, or other lineage determinants, may influence therapeutic resistance by modulating levels of ligand (e.g., heparin-binding EGF (HB-EGF)), receptor tyrosine kinases (RTKs; such as EGFR) or other downstream components of RTK signaling.

sensitivity although it may be related to the cell line used; in our hands, SKmel-28 cells have 11-fold more MITF than A375 cells (data not shown) and thus the A375 cells may have come to depend on SOX10 signaling to a greater extent. Instead of inducing resistance by SOX10 loss only, our study indicates that MITF loss only confers resistance in the presence of EGFR expression.

Our data indicate that RTK-induced resistance is dependent on ligand, and this broadens the picture of growth factors in drug resistance that was initially suggested in paracrine hepatocyte growth factor–induced primary BRAFi resistance (Straussman *et al.*, 2012; Wilson *et al.*, 2012). Our data are also consonant with a recent report that high EGFR-expressing cells often lack EGFR activation, presumably because of lack of ligands, and are still sensitive to BRAFi; thus, EGFR levels alone cannot be used as a biomarker of vemurafenib resistance (Gross *et al.*, 2014). Our results also suggest that ligand measurement in blood or other body fluid might be an eventual method to predict drug resistance clinically. It is intriguing that stable EGFR phosphorylation by constitutively active L858R mutant does not induce resistance, an insight from which might offer a more detailed understanding of EGFR-dependent resistance and strategies to overcome resistance.

In summary, lineage reprogramming appears to be directly coupled to RTK activation in the setting of therapeutic resistance. These comparative molecular studies provide a framework for understanding shifts in transcriptional states as resistance lesions emerge under drug selection. Efforts are now underway to recover useful therapeutic agendas to overcome these programs.

MATERIALS AND METHODS

Compounds, antibodies, and reagents

Vemurafenib, PLX4720, AZD6244, and U0126 were from Selleck Chemicals (Houston, TX). EGF, HB-EGF, and p-RTK arrays were purchased from R&D (Minneapolis, MN). Doxycycline was from Clontech (Mountain View, CA). Antibodies against p-EGFR, EGFR, BRAF, p-MEK. MEK, p-ERK, ERK, p-AKT, AKT, GAPDH, and α-tubulin were from Cell Signaling (Danvers, MA). CellTiter-Glo cell viability assay was from Promega (Madison, WI). AlamarBlue cell viability reagent was from Life Technologies (Grand Island, NY). Human phospho-RTK array kit was from R&D Systems. The siRNA against MITF and nontargeting control siRNA were from GE Dharmacon (Lafayette, CO).

Long-term cell proliferation assays

Cells were seeded into 6-well plates (1×10^4 cells per well) and cultured both in the absence and presence of drugs as indicated. After 10–15 days, cells were fixed with paraldehyde and stained with 1% crystal violet for 10 minutes. The plates were then washed with ddH_2O and dried in air before photographed.

Drug treatment and cell viability assay

Cell viability was determined by AlamarBlue (Life Technologies) fluorescence assay and CellTiter-Glo (Promega) luminescence assay. Approximately 12 hours before drug treatment, cells were seeded at a density of 3,000 cells (100 µl) per well in a 96-well plate. The plates were incubated with drugs for 48 hours. To each well, 10 µl of AlamarBlue was added and incubated for 3 hours at 37 °C. AlamarBlue is fluorescent substrates reduced by mitochondrial enzyme activity in viable cells. Alternatively, 30 µl of CellTiter-Glo was added to each well and incubated, protected from light on an orbital shaker, for 10 minutes. CellTiter-Glo contains luciferase that catalyzes the oxygenation of luciferin (creating light) according to the amount of adenosine triphosphate present. Fluorescence or luminescence intensity was determined using a Molecular Devices (Sunnyvale, CA) plate reader with an excitation filter centered on 540 nm and an emission filter centered on 590 nm or with an integration time of 500 ms and measuring total light emitted, respectively. GI_{50}s were calculated using the software CompuSyn (http://www.combosyn.com).

Stable infections

Lentiviral transduction was used to alter the levels of MITF. Lentiviral supernatant was produced by transient transfection of HEK293T cells (ATCC, Manassas, VA) using lipofectamine (Life Technologies), according to the manufacturer's instructions. The viral-containing supernatants were harvested 48 hours after transfection and filtered through a 0.45 µm filter unit. To transduce melanoma cells with lentivirus, logarithmically growing melanoma cells were seeded at a density of 2×10^5 cells per well in 6-well plates. A total of 0.5 ml of lentivirus suspension and 8 µg ml^{-1} of polybrene were added to DMEM with 10% fetal bovine serum in a total volume of 1 ml. Cells were incubated at 37 °C for 12 hours before removing the medium and replacing with 2 ml of fresh DMEM for expansion of the transductants. Cells were selected with puromycin at 1.5 µmol l^{-1} for another 5 days before further experiments.

Protein lysate preparation and immunoblots

Cells were seeded in medium containing 10% fetal bovine serum for 24 hours, and then washed with phosphate-buffered saline and lysed with RIPA buffer supplemented with Halt protease inhibitor cocktail (Thermo Scientific, Rockford, IL). Equal amounts of protein (5–20 µg) were loaded onto 4–20% SDS polyacrylamide mini-gels (Bio-Rad, Hercules, CA) and transferred to polyvinylidene difluoride membranes. After being blocked in 5% milk in Tris-buffered saline–Tween for 1 hour, blots were incubated with primary antibodies overnight, followed by horseradish peroxidase–conjugated secondary antibody (1:5,000) for 45 minutes. Antigen–antibody complexes were detected by enhanced chemiluminescence. Human p-RTK arrays were performed according to the manufacturer's instructions.

Melanoma patient tumor samples

Human melanoma specimens (all BRAF V600 mutated) were obtained from patients undergoing treatment with vemurafenib, dabrafenib, or trametinib in accordance with a protocol approved by the MGH institutional review board. All patients provided written informed consent for analysis, as approved by the Dana-Farber/Harvard Cancer Center Institutional Review Board (DF/HCC Protocol 11-181).

RNA isolation and reverse transcriptase–PCR

RNA isolation from cell lines harvested with TRIzol reagent (Invitrogen, Carlsbad, CA) according to the manufacturer's instructions. Complementary DNA (cDNA) synthesis was performed with Maxima Universal First-Strand cDNA Synthesis Kit (K1661, Thermo Scientific, Rockford, IL) according to the manufacturer's instructions. The cDNA was obtained by reverse transcription using High-Capacity cDNA Reverse Transcription kit (Applied Biosystems, Waltham, MA) according to the manufacturer's instructions. Levels of individual genes were quantified using a TaqMan Gene Expression Assays (Life Technologies) as previously described (Yang *et al.*, 2006): EGFR (Hs01076078_m1), EGF (Hs01099999_m1), HB-EGF (Hs00181813_m1), MITF (Hs01117294_m1), TCF4 (Hs00162613_m1), MIR211 (Hs04231471_s1), TGFA (Hs00608187_m1), SOX10 (Hs00366918_m1), BCL2 (Hs00608023_m1), PAX3 (Hs00240950_m1), LEF1 (Hs01548150_m1), CREB1 (Hs00231713_m1), and NRG1 (Hs00247620_m1). Human GUSB (4333767 T, Life Technologies, Grand Island, NY) was used as an endogenous control. Primer sequences for MITF-M were from Dynek *et al.* (2008). Real-time PCR was performed using the LightCycler480 (Roche, Indianapolis, IN) at 95 °C for 10 minutes for denaturation and then 95 °C for 10 seconds and 60 °C to 62 °C for 50 seconds for 45 cycles. The normalized, relative levels of the genes between samples were expressed as the $\log_2$ ratio (e.g., $-10 = 2^{-10} = 1{,}024$-fold reduction in expression in sample 1 vs. sample 2).

CONFLICT OF INTEREST

The authors state no conflict of interest.

ACKNOWLEDGMENTS

This work was supported in part by the National Institutes of Health (K24 CA149202, P01CA163222, 5T32CA071345, and 5T32AR007098), the American Skin Association, and the generous donors to the MGH Millennium Melanoma Fund. The work was further supported by the Swedish Cancer Society, Swedish Research Council, Berta Kamprad Foundation, Gunnar Nilsson Cancer Foundation, and Gustav Vth Jubilee Foundation.

SUPPLEMENTARY MATERIAL

Supplementary material is linked to the online version of the paper at http://www.nature.com/jid

REFERENCES

Barretina J, Caponigro G, Stransky N *et al.* (2012) The Cancer Cell Line Encyclopedia enables predictive modelling of anticancer drug sensitivity. *Nature* 483:603–7

Corcoran RB, Ebi H, Turke AB *et al.* (2012) EGFR-mediated re-activation of MAPK signaling contributes to insensitivity of BRAF mutant colorectal cancers to RAF inhibition with vemurafenib. *Cancer Discov* 2:227–35

Dynek JN, Chan SM, Liu J *et al.* (2008) Microphthalmia-associated transcription factor is a critical transcriptional regulator of melanoma inhibitor of apoptosis in melanomas. *Cancer Res* 68:3124–32

Furumura M, Potterf SB, Toyofuku K *et al.* (2001) Involvement of ITF2 in the transcriptional regulation of melanogenic genes. *J Biol Chem* 276: 28147–54

Garraway LA, Widlund HR, Rubin MA *et al.* (2005) Integrative genomic analyses identify MITF as a lineage survival oncogene amplified in malignant melanoma. *Nature* 436:117–22

Girotti MR, Pedersen M, Sanchez-Laorden B *et al.* (2013) Inhibiting EGF receptor or SRC family kinase signaling overcomes BRAF inhibitor resistance in melanoma. *Cancer Discov* 3:158–67

Gross A, Niemetz-Rahn A, Nonnenmacher A *et al.* (2014) Expression and activity of EGFR in human cutaneous melanoma cell lines and influence of vemurafenib on the EGFR pathway. *Target Oncol* 10:77–84

Hari Kishore A, Li XH, Word RA (2012) Hypoxia and PGE(2) regulate MiTF-CX during cervical ripening. *Mol Endocrinol* 26:2031–45

Itoh Y, Joh T, Tanida S *et al.* (2005) IL-8 promotes cell proliferation and migration through metalloproteinase-cleavage proHB-EGF in human colon carcinoma cells. *Cytokine* 29:275–82

Ji Z, Njauw CN, Taylor M *et al.* (2012) p53 rescue through HDM2 antagonism suppresses melanoma growth and potentiates MEK inhibition. *J Invest Dermatol* 132:356–64

Johannessen CM, Boehm JS, Kim SY *et al.* (2010) COT drives resistance to RAF inhibition through MAP kinase pathway reactivation. *Nature* 468:968–72

Johannessen CM, Johnson LA, Piccioni F *et al.* (2013) A melanocyte lineage program confers resistance to MAP kinase pathway inhibition. *Nature* 504: 138–42

Konieczkowski DJ, Johannessen CM, Abudayyeh O *et al.* (2014) A melanoma cell state distinction influences sensitivity to MAPK pathway inhibitors. *Cancer Discov* 4:816–27

Nazarian R, Shi H, Wang Q *et al.* (2010) Melanomas acquire resistance to B-RAF(V600E) inhibition by RTK or N-RAS upregulation. *Nature* 468: 973–7

Poulikakos PI, Persaud Y, Janakiraman M *et al.* (2011) RAF inhibitor resistance is mediated by dimerization of aberrantly spliced BRAF(V600E). *Nature* 480: 387–90

Prahallad A, Sun C, Huang S *et al.* (2012) Unresponsiveness of colon cancer to BRAF(V600E) inhibition through feedback activation of EGFR. *Nature* 483: 100–3

Shi H, Moriceau G, Kong X *et al.* (2012) Melanoma whole-exome sequencing identifies (V600E)B-RAF amplification-mediated acquired B-RAF inhibitor resistance. *Nat Commun* 3:724

Smith MP, Ferguson J, Arozarena I *et al.* (2013) Effect of SMURF2 targeting on susceptibility to MEK inhibitors in melanoma. *J Natl Cancer Inst* 105:33–46

Straussman R, Morikawa T, Shee K *et al.* (2012) Tumour micro-environment elicits innate resistance to RAF inhibitors through HGF secretion. *Nature* 487:500–4

Sun C, Wang L, Huang S *et al.* (2014) Reversible and adaptive resistance to BRAF(V600E) inhibition in melanoma. *Nature* 508:118–22

Villanueva J, Vultur A, Lee JT *et al.* (2010) Acquired resistance to BRAF inhibitors mediated by a RAF kinase switch in melanoma can be overcome by cotargeting MEK and IGF-1R/PI3K. *Cancer Cell* 18:683–95

Wilson BJ, Saab KR, Ma J *et al.* (2014) ABCB5 maintains melanoma-initiating cells through a proinflammatory cytokine signaling circuit. *Cancer Res* 74: 4196–207

Wilson TR, Fridlyand J, Yan Y *et al.* (2012) Widespread potential for growth-factor-driven resistance to anticancer kinase inhibitors. *Nature* 487:505–9

Yadav V, Zhang X, Liu J *et al.* (2012) Reactivation of mitogen-activated protein kinase (MAPK) pathway by FGF receptor 3 (FGFR3)/Ras mediates resistance to vemurafenib in human B-RAF V600E mutant melanoma. *J Biol Chem* 287:28087–98

Yang G, Zhang G, Pittelkow MR *et al.* (2006) Expression profiling of UVB response in melanocytes identifies a set of p53-target genes. *J Invest Dermatol* 126:2490–506